

3. W. Kabsch, H. G. Mannherz, D. Suck, E. F. Pai, K. C. Holmes, *Nature* **347**, 37 (1990).  
 4. P. J. McLaughlin, J. T. Gooch, H. G. Mannherz, A. G. Weeds, *Nature* **364**, 685 (1993).  
 5. R. C. Robinson et al., *Science* **286**, 1939 (1999).  
 6. C. E. Schutt, J. C. Myslik, M. D. Rozycki, N. C. Goonesekere, U. Lindberg, *Nature* **365**, 810 (1993).  
 7. W. Kabsch, K. C. Holmes, *Faseb J.* **9**, 167 (1995).  
 8. J. H. Hurley, *Annu. Rev. Biophys. Biomol. Struct.* **25**, 137 (1996).  
 9. D. Pantaloni, C. Le Clairche, M.-F. Cartier, *Science* **292**, 1502 (2001).  
 10. C. Combeau, M.-F. Cartier, *J. Biol. Chem.* **263**, 17429 (1988).  
 11. P. G. Allen, L. E. Laham, M. Way, P. A. Janmey, *J. Biol. Chem.* **271**, 4665 (1996).  
 12. A. Orlova, E. H. Egelman, *J. Mol. Biol.* **227**, 1043 (1992).  
 13. L. D. Belmont, A. Orlova, D. G. Drubin, E. H. Egelman, *Proc. Natl. Acad. Sci. U.S.A.* **96**, 29 (1999).  
 14. K. C. Holmes, D. Popp, W. Gebhard, W. Kabsch, *Nature* **347**, 44 (1990).  
 15. A. Orlova, E. H. Egelman, *J. Mol. Biol.* **232**, 334 (1993).  
 16. S. Y. Khaitlina, J. Moraczewska, H. Strzelecka-Golaszewska, *Eur. J. Biochem.* **218**, 911 (1993).  
 17. A. Muhrad, P. Cheung, B. C. Phan, C. Miller, E. Reister, *J. Biol. Chem.* **269**, 11852 (1994).  
 18. Y. S. Borovikov, J. Moraczewska, M. I. Khoroshev, H. Strzelecka-Golaszewska, *Biochim. Biophys. Acta* **1478**, 138 (2000).  
 19. E. Kim, M. Motoki, K. Seguro, A. Muhrad, E. Reister, *Biophys. J.* **69**, 2024 (1995).  
 20. J. Moraczewska, H. Strzelecka-Golaszewska, P. D. J. Moens, C. G. dos Remedios, *Biochem. J.* **317**, 605 (1996).  
 21. J. Moraczewska, B. Wawro, K. Seguro, H. Strzelecka-Golaszewska, *Biophys. J.* **77**, 373 (1999).  
 22. Actin was prepared and labeled (26) at Cys<sup>374</sup> with TMR from Molecular Probes. Briefly, G-actin (~6 mg/ml) in G-buffer was reacted overnight at 4°C (with stirring) with a two- to threefold molar excess of TMR, dissolved in dimethylformamide. The labeling reaction was stopped with dithiothreitol, after which the sample was exhaustively dialyzed against F-buffer (40 mM NaCl, 2 mM MgCl<sub>2</sub> added to G-buffer). Any polymerized, unreacted actin (about 5%) was removed by centrifugation at 100,000g for 30 min. The labeling ratio of the remaining TMR-actin was determined from the actin concentration (26) and the TMR concentration, which was calculated from the absorbance at the 557-nm peak with an extinction coefficient determined to be  $\epsilon = 1.06 \times 10^5 \text{ M}^{-1} \text{ cm}^{-1}$ . The labeling ratio was always between 0.9 and 1.0.  
 23. Crystals of TMR-labeled rabbit skeletal actin were obtained at 20°C by hanging drop vapor diffusion. In a typical experiment, 2  $\mu\text{l}$  of TMR-actin (6 mg/ml) were mixed with 2  $\mu\text{l}$  of a reservoir solution containing 22% polyethylene glycol 2000 monomethyl ether, 10 mM tris (pH 7.0), and 200 mM calcium acetate. A series of seeding experiments on sitting drop plates is usually required to obtain crystals suitable for diffraction. Data collection was performed at 100 K from crystals frozen in propane after addition of 13% ethylene glycol to the crystallization buffer. Two data sets were collected at IMCA-CAT beamline 17-ID and BioCARS beamline 14-BM-C at the Advanced Photon Source, Argonne, IL (Table 1). The data sets were processed with the HKL2000 package (27). The structure was determined by molecular replacement with the actin-DNase I structure as a search model with the program AMoRe (28). The model was refined to 1.54 Å resolution with the programs wARP (29) and Refmac from the CCP4 suite of programs (30). Table 1 summarizes the data collection, refinement, and model quality statistics.  
 24. R. Dominguez, Y. Freyroz, K. M. Trybus, C. Cohen, *Cell* **94**, 559 (1998).  
 25. J. E. Estes, L. A. Selden, H. J. Kinoshita, L. C. Gershman, *J. Muscle Res. Cell Motil.* **13**, 272 (1992).  
 26. P. Graceffa, *J. Biol. Chem.* **275**, 17143 (2000).  
 27. Z. Otwinowski, W. Minor, *Methods Enzymol.* **276**, 307 (1997).  
 28. J. Navaza, *Acta Crystallogr.* **A50**, 157 (1994).

29. A. Perrakis, R. Morris, V.S. Lamzin, *Nature Struct. Biol.* **6**, 458 (1999).  
 30. CCP4, *Acta Crystallogr.* **D50**, 760 (1994).  
 31. We thank H. Paulus, K. Langsetmo, and Z. Grabarek for critical reading of the manuscript. Supported by NIH grants R01 AR46524 (R.D.), P01 AR41637 (P.G.), and March of Dimes grant 5-FY99-774 (R.D.). Use of the Advanced Photon Source was supported by the U.S. Department of Energy, Basic Energy Sciences, Office of

Science, under contract W-31-109-Eng-38. Use of the BioCARS facilities was supported by NIH grant RR07707. Use of the IMCA-CAT facilities was supported by the companies of the Industrial Macromolecular Crystallography Association and the Illinois Institute of Technology. Coordinates have been deposited at the Protein Data Bank (entry code 1J6Z).

8 February 2001; accepted 1 June 2001

## Tauopathy in *Drosophila*: Neurodegeneration Without Neurofibrillary Tangles

Curtis W. Wittmann,<sup>1</sup> Matthew F. Wszolek,<sup>1</sup> Joshua M. Shulman,<sup>1</sup> Paul M. Salvaterra,<sup>2</sup> Jada Lewis,<sup>3</sup> Mike Hutton,<sup>3</sup> Mel B. Feany<sup>1\*</sup>

The microtubule-binding protein tau has been implicated in the pathogenesis of Alzheimer's disease and related disorders. However, the mechanisms underlying tau-mediated neurotoxicity remain unclear. We created a genetic model of tau-related neurodegenerative disease by expressing wild-type and mutant forms of human tau in the fruit fly *Drosophila melanogaster*. Transgenic flies showed key features of the human disorders: adult onset, progressive neurodegeneration, early death, enhanced toxicity of mutant tau, accumulation of abnormal tau, and relative anatomic selectivity. However, neurodegeneration occurred without the neurofibrillary tangle formation that is seen in human disease and some rodent tauopathy models. This fly model may allow a genetic analysis of the cellular mechanisms underlying tau neurotoxicity.

Alzheimer's disease is characterized by the accumulation of abnormally phosphorylated and aggregated forms of the microtubule-binding protein tau. Aggregates of tau form intracytoplasmic neuronal inclusions known as neurofibrillary tangles. The formation of neurofibrillary tangles closely parallels the progression and anatomic distribution of neuronal loss in Alzheimer's disease (1), suggesting that these lesions play a role in the pathogenesis of the disorder. Mutations in the human tau gene are found in autosomal dominant neurodegenerative disorders linked to chromosome 17 (2). These familial disorders and similar sporadic diseases (3) are also characterized by extensive neurofibrillary pathology and are often termed "tauopathies." The autosomal dominant inheritance in familial tauopathies and the accumulation of abnormal tau protein in all tauopathies suggest a toxic dominant pathogenic mechanism.

To create a genetic model of these tauopathies, we expressed wild-type and mutant forms of human tau in *Drosophila melano-*

*gaster*. Wild-type tau or Arg<sup>406</sup> → Trp (R406W) mutant tau, an isoform associated with an early onset, familial form of dementia, was first expressed in a panneuronal pattern (elav-GAL4) (4). The life-span of the flies was moderately shortened by wild-type tau and severely shortened by the mutant tau (Fig. 1). Western blot analysis revealed that the R406W 1 transgenic line expressed 0.8-fold less tau than the tau wild-type 1 transgenic line, indicating that the mutant tau was substantially more toxic than wild-type tau. All quantitative comparisons between wild-type and mutant tau in subsequent analyses were carried out with the tau wild-type 1 and R406W 1 transgenic lines. Tau wild-type 2 transgenic flies expressed 1.3-fold more tau than the tau wild-type 1 line. R406W 2 transgenics expressed 1.5-fold more tau than tau wild-type 1 flies. Effects of both wild-type and R406W mutant human tau on life-span were therefore dosage sensitive. Total fly brain homogenate from transgenic tau wild-type 1 animals contained about 0.5-fold less human tau protein per mg of protein than control human brain homogenate, indicating that transgenic animals did not have massive overexpression of human tau.

To determine if early death correlated with neurodegeneration, we examined the brains of tau transgenics. We first demonstrated that the nervous system of our transgenic flies was normal in newly eclosed

<sup>1</sup>Department of Pathology, Division of Neuropathology, Brigham and Women's Hospital and Harvard Medical School, 221 Longwood Avenue, Room 514, Boston, MA 02115, USA. <sup>2</sup>Division of Neurosciences, Beckman Research Institute of the City of Hope, Duarte, CA 91010, USA. <sup>3</sup>Mayo Clinic Jacksonville, Jacksonville, FL 32224, USA.

\*To whom correspondence should be addressed: E-mail: mel\_feany@hms.harvard.edu

young adult flies (Fig. 2, A and B) (5). Tau transgenics were compared with controls for presence and appropriate organization of major projection systems and anatomic structures and for preservation of appropriate cortical cell numbers and neuropil volumes. No abnormalities were detected. The normal histologic appearance of tau transgenic brains in 1-day-old adults correlated with grossly normal behavior of young transgenic animals. These results are consistent with normal development and anatomy of mice transgenic for human tau (6–8).

In contrast to the young tau transgenics, aged flies showed clear histologic abnormalities in the brain. Aged flies expressing tau showed obvious vacuolization and degeneration of cells in the cortex (Fig. 2, D to I). There was also a modest increase in neuropil vacuolization (Fig. 2D, arrowheads). Normal aged flies showed some increase in neuropil

vacuoles with age, although less in extent and size than tau transgenics, even in much older flies (Fig. 2, C and E). Vacuolar pathology is not a prominent feature of Alzheimer's disease or frontotemporal dementia; however, neurodegeneration in *Drosophila* is commonly accompanied by vacuoles (9–11). Vacuolar pathology may reflect the relatively rapid tempo of neurodegeneration in flies. Quantitative experiments revealed that degeneration was progressive and was more severe in flies expressing mutant tau (Fig. 2E). All aged tau transgenic flies showed obvious degeneration, indicating that the phenotype was fully penetrant.

We next evaluated the flies with a variety of conformation and phosphorylation-specific antibodies that have been used to detect abnormal tau in disease states. The Alz50 and MC1 monoclonal antibodies recognize abnormal tau conformations present in degenerative disease tissue, but not in normal human adult brain (12). The phosphorylation-specific antibodies AT8, 12E8, AT100, and AT180 preferentially recognize tau phosphorylations characteristic of disease states. The abnormal conformational changes and phosphorylations identified by these antibodies were all present in brains of flies expressing either wild-type or mutant human tau. Immunoreactivity for Alz50, MC1, 12E8, AT100, and AT180 increased as the flies aged, whereas immunoreactivity for a human-specific polyclonal tau antibody remained constant as the animals aged. No cross reactivity with endogenous fly tau was observed with any of the antibodies in nontransgenic flies. These results demonstrate that abnormal human tau accumulated with age in the brains of tau transgenic flies. Abnormal tau was also

concentrated in areas of neurodegeneration (Fig. 2H). The cortex and neuropil adjacent to degenerating cells and vacuoles commonly, although not invariably, showed localized or increased immunoreactivity for Alz50, MC1, 12E8, AT100, and AT180.

To determine if tau formed neurofibrillary tangles in transgenic flies, we performed electron microscopy (EM). Although degenerating cells were readily identified (Fig. 2I), there was no evidence of large filamentous aggregates (neurofibrillary tangles). This EM analysis was performed on flies at multiple ages that expressed wild-type or R406W mutant tau in all neurons (*elav-GAL4*) or specifically in cholinergic neurons (*Cha-GAL4*) (13). We examined a total of 359 degenerating neurons, representing cells at various stages of degeneration, and found no large filamentous aggregates. To confirm these results, we created transgenic flies that expressed Val<sup>337</sup> → Met (V337M) mutant tau, an additional mutation associated with early onset, familial dementia (2). These flies showed neurodegeneration and a tau immunostaining profile, similar to that of wild-type and R406W mutant tau transgenics. An additional 159 degenerating cells were examined in V337M transgenics. No large filamentous aggregates were identified. In an attempt to identify filamentous tau, sarcosyl insoluble tau from wild-type, R406W, and V337M transgenic fly brains was prepared and examined by immunoelectron microscopy (14–16). Tau-immunoreactive filaments were not identified. In sum, these results suggest that tau-induced neurodegeneration does not require large filamentous tau aggregates. However, we cannot exclude the presence of infrequent neurofibrillary tangles, scattered tau

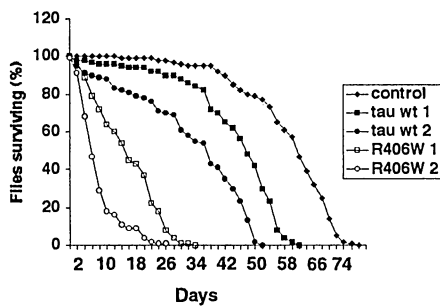
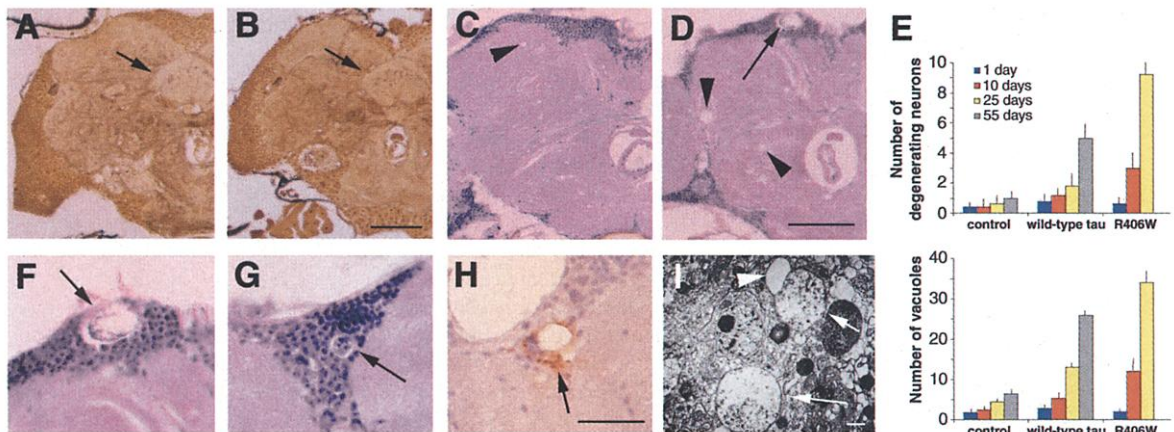


**Fig. 1.** Tau transgenic flies die prematurely. At least 250, and usually more than 350, flies of each genotype were collected at 1 day after eclosion and assayed for longevity (10). Control genotype: *elav-GAL4/+*. Experimental genotypes: *elav-GAL4/+; UAS-wt tau/+* and *elav-GAL4/+; UAS-R406W tau/+*.

**Fig. 2.** Expression of human tau induces neurodegeneration in transgenic flies. (A and B) Silver stained sections of 1-day-old tau transgenic flies show normal anatomy. Arrows demonstrate appropriately formed fan-shaped bodies. Scale bar, 50  $\mu$ m. (A) Control genotype: *elav-GAL4/+*. (B) Experimental genotype: *elav-GAL4/+; UAS-R406W 1 tau/+*. (C and D) Neurodegeneration is apparent in aged tau transgenics (D), but not aged controls (C). Arrow shows degenerating cells (C) and (D)]. Scale bar, 50  $\mu$ m. (C) Control genotype: *elav-GAL4/+*, 60 days. (D) Experimental genotype: *elav-GAL4/+; UAS-R406W 2 tau/+*, 20 days. (E) Quantitation of degenerating cells (top) and vacuolization (bottom). Control genotype: *elav-GAL4/+*. Experimental genotypes: *elav-GAL4/+; UAS-wt tau 1/+* and *elav-GAL4/+; UAS-R406W 1 tau/+*. (F and G) Higher magnification of degenerating neurons



(arrows) in aged tau transgenic flies. Genotype: *elav-GAL4/+; UAS-R406W 2 tau/+*, 20 days. (H) Abnormal tau surrounding a region of degeneration in a transgenic fly as shown by MC1 immunostaining (arrow). Genotype: *elav-GAL4/+; UAS-R406W 1 tau/+*, 10 days. Scale bar (F to H), 25  $\mu$ m. (I) Electron micrograph showing degenerating neurons in a tau transgenic. Arrows point to abnormal, swollen nuclei, and the arrowhead points to a vacuole. Genotype: *elav-GAL4/+; UAS-wt tau 1/+*, 45 days. Scale bar, 0.5  $\mu$ m.

filaments, or small protofibril species.

A key feature of all human neurodegenerative diseases is specificity for particular neuronal subpopulations. We therefore generated flies that selectively expressed tau in cholinergic neurons, which are particularly vulnerable to neurodegeneration in Alzheimer's disease and can be affected in tauopathies (17). Cholinergic neurons of the optic lamina immunostained with antibody AT8 appeared normal in 1-day-old (after eclosion) transgenic flies expressing wild-type or R406W mutant tau (Fig. 3A). In contrast, immunostaining at 30 days revealed widespread vacuolization and loss of cholinergic neurons (Fig. 3B). Similar results were observed in cholinergic neurons of the central body complex (Fig. 3, C and D). Quantitation of cholinergic neuronal loss in the lamina (Fig. 3E) demonstrated that neuronal loss was progressive and was worse in flies expressing mutant versus wild-type human tau (18). Expression of an unrelated protein linked to neurodegenerative diseases, human  $\alpha$ -synuclein, was not toxic to cholinergic neurons (Fig. 3E).  $\alpha$ -synuclein shows relative selectivity for dopaminergic neurons in Parkinson's disease and transgenic flies (19).

To further investigate the cell type specificity of tau for cholinergic neurons, we used an antibody to acetylcholine to stain cholinergic terminals in flies expressing tau in a panneural pattern (*elav-GAL4*). The number of cholinergic terminals was the same in 1-day-old (after eclosion) control flies and flies expressing wild-type or R406W mutant tau. In contrast, terminal staining was markedly diminished in aged transgenic flies (Fig. 3, F to H), especially in flies expressing R406W mutant tau (Fig. 3H). In contrast, no loss of terminal staining was observed in aged flies expressing  $\alpha$ -synuclein in a panneural pattern (*elav-GAL4*). Similar experiments were performed with an antibody against tyrosine hydroxylase that specifically recognizes dopaminergic cell bodies and pro-

cesses. No loss of tyrosine hydroxylase-positive terminals was identified in aged tau transgenics. Motor neurons were also relatively preserved in tau transgenic flies (18, 20, 21).

Specificity for cholinergic neurons in human tau transgenic flies is relative rather than absolute. The degree of histologic degeneration in panneural expressing flies (*elav-GAL4*) exceeded that seen in cholinergic neuron-expressing flies (*Cha-GAL4*), suggesting that additional cell populations degenerated. Expression of wild-type or mutant human tau in cholinergic neurons did not affect life-span, as did expression of tau in a panneural pattern (Fig. 1). In addition, expressing mutant human tau in photoreceptors was toxic and produced a rough eye phenotype (21). The rough eye phenotype has been used successfully in many *Drosophila* second site modifier screens and may facilitate use of the *Drosophila* tauopathy model to delineate cellular pathways mediating tau neurotoxicity.

In summary, we have created a *Drosophila* model of tauopathies by expressing human tau in fruit flies. Our model faithfully replicates a number of features of the human disorders: adult onset, progressive neurodegeneration, accumulation of abnormal tau, and early death. However, we did not see the large filamentous tau aggregates that are observed in human disease and other experimental models of tauopathy (2, 8, 22, 23).

The formation of large intraneuronal protein aggregates characterizes many neurodegenerative syndromes, including the two most common disorders, Alzheimer's disease and Parkinson's disease. A common mechanism of toxicity has been postulated in these diseases: Large aggregates act either as physical barriers to transport and other essential neuronal functions or have direct toxic effects on cells. Our results argue that, at least in the case of tau, neurotoxicity instead depends on protein alterations that occur before the for-

mation of large aggregates. In flies, neurodegeneration correlates with the abnormal configurations and phosphorylations of tau that commonly precede neurofibrillary tangle formation (12, 24), suggesting that these early modifications are the toxic substrates of tauopathies. The observation that some patients with tau mutations and frontotemporal dementia have extensive neurodegeneration, but sparse neurofibrillary tangles (25), is also consistent with a dissociation between tangle formation and tau neurotoxicity. Alternatively, the mechanism of toxicity in *Drosophila* may differ from that in human disease. *Drosophila* neurons differ from human neurons in potentially important respects. Fly neurons are on average smaller than vertebrate neurons, and they lack neurofilaments. If large cell size, neurofilament content, or other vertebrate-specific neuronal features are required for proper recapitulation of tauopathy mechanisms, the fly model will not be accurate. Although we cannot exclude this possibility, the enhanced biological toxicity of mutant tau, the degenerative nature of the pathology, and the selective accumulation of abnormal tau in areas of neuronal degeneration all argue that the mechanisms of tau neurotoxicity are conserved between flies and humans. Mechanisms of toxicity do appear conserved between human neurodegenerative diseases caused by polyglutamine expansions, such as Huntington's disease, and *Drosophila* models of these disorders (26–29). Given these homologies and a phenotype amenable to rapid screening, the fly tauopathy model can now be used to identify the molecular mechanisms that underlie tau neurotoxicity.

References and Notes

1. H. Braak, E. Braak, *Acta Neuropathol.* **82**, 239 (1991).
2. M. Hutton, *Ann. N.Y. Acad. Sci.* **920**, 63 (2000).
3. M. B. Feany, D. W. Dickson, *Ann. Neurol.* **40**, 139 (1996).

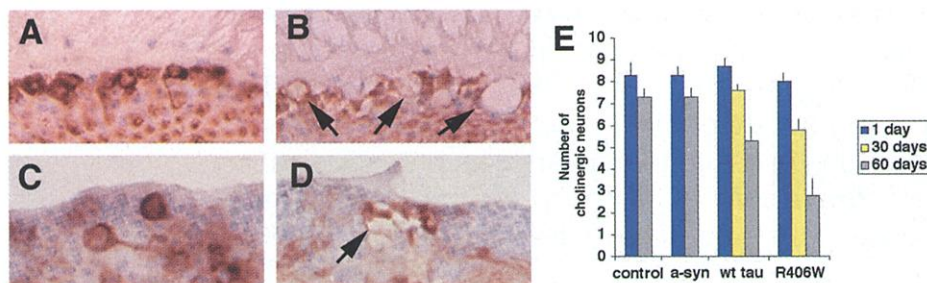


**Fig. 3.** Cholinergic neurons degenerate in tau transgenic flies. (A) Tau immunostaining shows normal appearing cholinergic neurons in the optic lamina of 1-day-old (after eclosion) flies. (B) Degeneration of lamina neurons in 30-day-old tau transgenic fly brain (arrows). (C) Cholinergic neurons in the central body complex in 1-day-old flies. (D) Degeneration of neurons in the same area in 30-day-old flies (arrow). (A to D) Genotype: *Cha-GAL4/+; UAS-R406W tau 2/+*. (E) Quantitation of cholinergic neuronal loss in the optic lamina. Control genotypes: *Cha-GAL4/+; UAS-lacZ/+* and *Cha-GAL4/+; UAS-A30P  $\alpha$ -synuclein/+*. Experiment-

tal genotypes: *Cha-GAL4/+; UAS-wt tau 1/+* and *Cha-GAL4/+; UAS-R406W tau 1/+*. (F to H) Acetylcholine staining shows loss of cholinergic terminals in aged flies expressing tau in a panneural pattern. Arrows indicate row of acetylcholine-immunoreactive terminals in the optic medulla. (F) Control. Genotype: *elav-GAL4/+*, 60 days. (G) Wild-type tau transgenic. Genotype: *elav-GAL4/+; UAS-wt tau 1/+*, 55 days. (H) Mutant tau transgenic. Genotype: *elav-GAL4/+; UAS-R406W tau 1/+*, 25 days. Arrowheads indicate degenerative vacuoles. Scale bar, 10  $\mu$ m.

## REPORTS

4. A. H. Brand, N. Perrimon, *Development* **118**, 401 (1993).
5. Heads from adult flies at 1 day after eclosion were fixed in formalin and embedded in paraffin, and 4- $\mu$ m frontal sections were prepared. Serial sections were cut through the entire brain, placed on a single glass slide, and stained with hematoxylin and eosin (H&E), Bielschowsky (Fig. 2, A and B), or bodian silver stains. H&E sections highlight the normal arrangement of basophilic neuronal and glial cell bodies in the outer cortical layer and the inner eosinophilic neuropil regions. Silver stains label axonal projections and demonstrate anatomic features. The quantitative analysis in Fig. 2E was performed on 4- $\mu$ m-thick paraffin sections stained with H&E. The number of degenerating neurons and the number of vacuoles measuring greater than 5  $\mu$ m in diameter were counted in five well-oriented frontal sections between the level of the fan-shaped body and the calyx of the mushroom body. Sections from at least five individual brains were examined per time point for each genotype.
6. J. P. Brion, G. Trem, J. N. Octave, *Am. J. Pathol.* **154**, 255 (1999).
7. T. Ishihara *et al.*, *Neuron* **24**, 751 (1999).
8. J. Lewis *et al.*, *Nature Genet.* **25**, 402 (2000).
9. P. E. Coombe, M. Heisenberg, *J. Neurogenet.* **3**, 135 (1986).
10. R. L. Buchanan, S. Benzer, *Neuron* **10**, 839 (1993).
11. D. Kretzschmar *et al.*, *J. Neurosci.* **17**, 7425 (1997).
12. G. A. Jicha, R. Bowser, I. G. Kazam, P. Davies, *J. Neurosci. Res.* **48**, 128 (1997).
13. K. Yasuyama, P. M. Salvaterra, *Microsc. Res. Tech.* **45**, 65 (1999).
14. Sarcosyl insoluble tau was prepared by standard methods (15, 16). Briefly, fly heads were homogenized in 10 volumes buffer and centrifuged for 20 min at 15,000g. The supernatant was brought to 1% *N*-lauroylsarcosinate, incubated for 1 hour at room temperature with shaking, and then further centrifuged for 1 hour at 100,000g. The resultant high-speed pellet was resuspended at 10  $\mu$ l per 50 mg of starting material. Tau was detected by immunoblot analysis in the sarcosyl insoluble fraction, and this sarcosyl insoluble fraction was subjected to immunoelectron microscopy. Control genotype: *elav-GAL4/+*. Experimental genotypes: *elav-GAL4/+; UAS-wt tau/+*, *elav-GAL4/+; UAS-R406W tau/+*, and *elav-GAL4/UAS-V337M tau/+*. All flies were 30 days old.
15. S. G. Greenberg, P. Davies, *Proc. Natl. Acad. Sci. U.S.A.* **87**, 5827 (1990).
16. M. Goedert, M. G. Spillantini, N. J. Cairns, R. A. Crowther, *Neuron* **8**, 159 (1992).
17. J. F. Geddes, A. J. Hughes, A. J. Lees, S. E. Daniel, *Brain* **116**, 281 (1993).
18. For analysis of specific neuronal subsets, we expressed wild-type and mutant tau using *Cha-GAL4* for cholinergic neurons and *D42-GAL4* for motor neurons. The *D42-GAL4* and *Cha-GAL4* lines produced equivalent amounts of  $\beta$ -galactosidase ( $\beta$ -Gal) when crossed to a GAL4 responsive  $\beta$ -Gal transgene (*UAS-lacZ*). A transgene encoding a marker protein (*UAS-lacZ* or *UAS-GFP*) was coexpressed to provide an independent method of identifying cholinergic or motor neurons. Cholinergic neurons in the optic lamina were immunostained for AT8,  $\beta$ -Gal, or green fluorescent protein (GFP), and the number of immunoreactive neurons per 60- $\mu$ m region of optic lamina (4- $\mu$ m-thick sections) was counted. Each time point and genotype represents the average of at least six separate retinas. For analysis of process staining with acetylcholine or tyrosine hydroxylase immunohistochemistry in panneural expressing flies (*elav-GAL4*), sections of control and transgenic fly brains were prepared and immunostained in parallel. Similar results were seen in at least three separate experiments.
19. M. B. Feany, W. W. Bender, *Nature* **404**, 394 (2000).
20. E. Yeh, K. Gustafson, G. L. Boulianne, *Proc. Natl. Acad. Sci. U.S.A.* **92**, 7036 (1995).
21. See supplementary data available at Science Online at [www.sciencemag.org/cgi/content/full/1062382/DC1](http://www.sciencemag.org/cgi/content/full/1062382/DC1).
22. T. Ishihara *et al.*, *Am. J. Pathol.* **158**, 555 (2001).
23. G. F. Hall, J. Yao, G. Lee, *Proc. Natl. Acad. Sci. U.S.A.* **94**, 4733 (1997).
24. G. A. Jicha, B. Berenfeld, P. Davies, *J. Neurosci. Res.* **55**, 713 (1999).
25. T. D. Bird *et al.*, *Brain* **122**, 741 (1999).
26. J. M. Warrick *et al.*, *Nature Genet.* **23**, 425 (1999).
27. P. Fernandez-Funez *et al.*, *Nature* **408**, 101 (2000).
28. H. Y. Zoghbi, H. T. Orr, *Annu. Rev. Neurosci.* **23**, 217 (2000).
29. M. B. Feany, *J. Neuropathol. Exp. Neurol.* **59**, 847 (2000).
30. We thank W. Bender for generous support, P. Davies and P. Seubert for valuable reagents, and H. Shing, D. Bowman, M. Slaney, C. Ridolfi, and A. Merola for excellent technical assistance. This work was funded by grants from the National Institute on Aging, the Howard Hughes Medical Institute, the McKnight Endowment Fund for Neuroscience (M.B.F.), and the NIH (W. Bender).

9 May 2001; accepted 1 June 2001  
 Published online 14 June 2001;  
 10.1126/science.1062382  
 Include this information when citing this paper.

# So instant, you don't need water...

## NEW! Science Online's Content Alert Service

There's only one source for instant updates on breaking science news and research findings: *Science's* Content Alert Service. This free enhancement to your *Science* Online subscription delivers e-mail summaries of the latest research articles published each Friday in *Science* – **instantly**. To sign up for the Content Alert service, go to *Science* Online – and save the water for your coffee.

**Science**  
[www.sciencemag.org](http://www.sciencemag.org)

For more information about Content Alerts go to [www.sciencemag.org](http://www.sciencemag.org). Click on Subscription button, then click on Content Alert button.